

UNCLASSIFIED

Defense Technical Information Center
Compilation Part Notice

ADP014098

TITLE: Investigation on the Capability of a Non Linear CFD Code to Simulate Wave Propagation

DISTRIBUTION: Approved for public release, distribution unlimited
Availability: Hard copy only.

This paper is part of the following report:

TITLE: Aging Mechanisms and Control. Symposium Part A - Developments in Computational Aero- and Hydro-Acoustics. Symposium Part B - Monitoring and Management of Gas Turbine Fleets for Extended Life and Reduced Costs [Les mecanismes vieillissants et le controle] [Symposium Partie A - Developpements dans le domaine de l'aeroacoustique et l'hydroacoustique numeriques] [Symposium Partie B ...

To order the complete compilation report, use: ADA415749

The component part is provided here to allow users access to individually authored sections of proceedings, annals, symposia, etc. However, the component should be considered within the context of the overall compilation report and not as a stand-alone technical report.

The following component part numbers comprise the compilation report:

ADP014092 thru ADP014141

UNCLASSIFIED

Investigation on the Capability of a Non Linear CFD Code to Simulate Wave Propagation

Pedro de la Calzada

Pablo Quintana

Manuel Antonio Burgos

ITP, S.A.

Parque Empresarial Fernando

avenida Castilla 2

Edificio Japon

E-28830 San Fernando de Henares, Madrid

Spain

Abstract

The potential wave propagation is described by defining the driving parameters of the propagation characteristics. Then a parametric study with a non linear code is performed in order to define the mesh refinement needed to obtain a sufficient accuracy in the predictions of inflow and outflow perturbation propagation. The results are compared with a linear version of the code as well as with a linear code for flat plate response showing the good behaviour of the non linear code. As additional test cases, the behaviour of the code for simulating the response of a cascade of flat plates to potential disturbances is investigated. Results from the different linear and non linear codes are also compared. Different cases are investigated including one with large resonances, which is shown to be the most difficult case to be predicted, in special the resonance peaks as well as the trailing edge region regarding the wave phase behaviour.

1 Introduction

The principal aircraft and engine manufacturers in Europe are facing increasing pressure to reduce aircraft noise levels. Regarding the noise from engines, low pressure turbine (LPT) noise is becoming more important due to the decrease of jet noise with the high by pass ratio cycles and lower noise from the advanced design fans and negative scarfed intake angles. In a LPT, the interaction of unsteady flow with the turbine blading produces fluctuating forces along the blades and results in unwanted effects such as noise and forced vibration. Such excitations are mainly generated at multiples of the blade passing frequency and arise from a variety of sources. The two principal types of such interaction are usually referred to as potential flow and wake interaction. The former is associated with unsteady pressure variations generated by the upstream and downstream rows and could be of serious concern when the axial spacing between neighbouring blade rows are small or flow Mach numbers or excitation frequencies are high. The wake interaction is due to vortical perturbations generated by wakes convected from the viscous flow on upstream rows.

Trying to understand the generation of noise by the mechanisms above presented, simulation of unsteady aerodynamics with linear and nonlinear CFD codes is an ongoing activity within the turbomachinery industry. However, the accurate resolution of the unsteady aerodynamics and acoustics on low pressure turbines remains a formidable computational problem. This is due mainly to the spatial resolution required to accurately simulate the incoming waves (potential and vortical fluctuations) and the radiated cut-off and cut-on waves, even in the case that only the 2D problem is considered. Traditionally linear codes have been used in the simulation of unsteady flows in turbomachinery. This approach allows the use of relatively coarse meshes and they need less computational effort when compared with non linear Euler solvers. However they assume that perturbations are small when compared with steady variables and they need to solve a new set of equations for the unsteady variables. This approach has been taken by many authors ([1] and [2] among others).

A different approach is taken at ITP, where a non linear unstructured Navier Stokes solver is intended to be used for resolution of both the steady and unsteady aerodynamics and acoustics, that will allow the use

of only one code to solve both problems coupled. This seems to be the current approach taken by some other authors to simulate wake-boundary layer interaction [3] and to simulate potential interaction [4].

For this investigation an in-house code, with the non linear MU²S²T and linear MU²S²TL versions is used. An extensive investigation on the different parameters involved in the propagation of waves is being carried out with the objective to assess the mesh resolution requirement and the capability of the solver to accurately simulate wave propagation and unsteady response of blade rows.

The results will be presented in an step by step approach, from the different parameters involved in noise propagation to the comparison with analytical linear solution of a flat plate response to incoming disturbances.

2 Theoretical background of the wave propagation

The equation governing the unsteady velocity potential for small deviations for an uniform, isentropic and irrotational mean flow has the following expression.

$$\frac{\partial^2 \Phi}{\partial t^2} - 2 \cdot \frac{M}{c} \cdot \frac{\partial^2 \Phi}{\partial x \partial y} + (1 - M^2) \frac{\partial^2 \Phi}{\partial x^2} + \frac{\partial^2 \Phi}{\partial y^2} = 0 \quad (1)$$

that has expression of the type

$$\Phi = \sum \sum A_{n,j} e^{i(\omega_n t + k_{yj} y + k_{xn,j} x)} \quad (2)$$

as solution.

For turbomachinery kind of flow fields, the temporal and circumferential eigenvalues are

$$\omega_n = n\Omega \quad (3)$$

$$k_{yj} = \frac{2\pi j}{\lambda_y} \quad (4)$$

and a expression for the axial wave number

$$k_{xn,j} = \frac{M_x (k_{yj} M_y + \frac{\omega}{c}) \pm \sqrt{(k_{yj} M_y + \frac{\omega}{c})^2 - k_y (1 - M_x^2)}}{1 - M_x^2} \quad (5)$$

From (5), the resonance frequency can be defined as

$$\omega_r = \frac{ck_{yj}(1 - M^2)}{\sqrt{M_y \pm (1 - M_x^2)}} \quad (6)$$

defining the cut-off ratio as

$$\xi = \frac{\omega}{\omega_r} \quad (7)$$

Ratios higher than unity give, according to (5), the so call cut-on waves (waves propagating with constant amplitude), while ratios lower than unity give cut-off waves (exponentially decaying waves in axial direction).

For cut-on waves, the wavelength in axial direction can be defined

$$\lambda_x = \frac{2\pi}{k_{xn,j}} \quad (8)$$

for a propagation wave number

$$k = \frac{2\pi}{\sqrt{\lambda_x^2 + \lambda_y^2}} \quad (9)$$

3 Wave propagation simulation with CFD

From the expressions derived above, it can be easily seen that the physical characteristics of the propagation of a potential wave depends on the following parameters.

$$\Phi = f(U_x, U_y, \rho, T, R_g, \gamma, \mu, \omega, \lambda_y) \quad (10)$$

Where ψ stands for any unsteady fluid variable.

That involves longitudes, time, mass, temperature and angular quantities. If the speed of sound c , R_g , the wave length λ_y and the density ρ are taken for nondimensionalization, the problem is reduced to

$$\Phi = f(M_x, M_y, \xi, Re) \quad (11)$$

M_x and M_y are mach number in x and y direction, ξ is the cut-off ratio, or the ratio of axial to circumferential wavelength (that involves also the Mach numbers, but gives the axial propagation characteristics), and Re states for the Reynolds number based in the wavelength λ_y .

If the propagation is to be simulated with a CFD code, parameters implicit to the code will be also relevant to the problem. These parameters have to do with the time and space discretization as well as the scheme used for the stabilization of the system of equations.

$$\Phi = f(M_x, M_y, \xi, Re, CFL, \sigma_2, \sigma_4) \quad (12)$$

Other set of characteristics in the simulation of the wave propagation are the parameters depending on the definition of the mesh employed for the computation, typically N_y cells in y direction and N_x cells in axial direction. For wave propagation, is of interest to define n_y and n_x as the points per circumferential and axial wavelength respectively.

$$\Phi = f(M_x, M_y, \xi, Re, CFL, \sigma_2, \sigma_4, n_x, n_y) \quad (13)$$

In real turbomachinery problems, potential and vortical wakes perturbations are present. As this paper is focused on potential disturbances, that are not affected by definition by the Reynolds number, no analysis on this parameter will be done here. Regarding the effect of the artificial viscosity parameters included in the code for stabilization, namely σ_2 and σ_4 , their effect will not be investigated since has been already investigated on the same code by Corral et al. [6]. Nevertheless some conclusions of their work will be used and commented here. The only effect of the CFL number on wave propagation is computing time and no further results on the simulation will be presented here.

Therefore the parametric investigation will cover the dependence of the results on the following parameters:

$$\Phi = f(M_x, M_y, \xi, n_x, n_y) \quad (14)$$

In addition, studies on the effect of the quasi-structured versus fully unstructured meshes has been performed. For this analysis, quasi-structured meshes composed of quadrilateral cells with one preferred diagonal direction have been used.

In the Figure 1, the results for a potential perturbation imposed in the outlet, with a ξ ratio of 5.0, $M=0.4$ are displayed. Due to the high propagation angle of the wave, the simulation presents a low number of

points per axial wavelength and the results present a deficient prediction of the cut-on wave (the mesh has 80 points in circumferential direction and approximately 10 points per axial wavelength). Furthermore the Figure 1 shows that there is some effect of the chosen diagonal direction on the damping of the propagating wave.

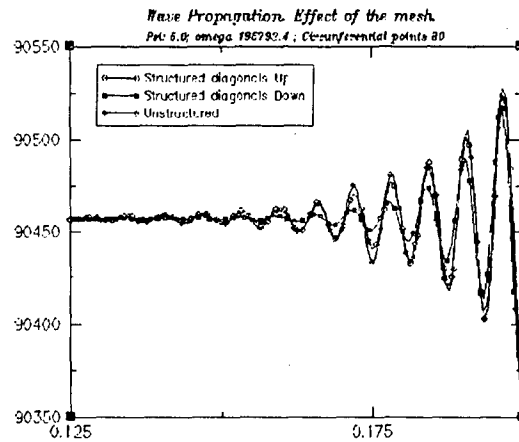


Figure 1: Effect of the mesh. $\xi: 5.0$, $\omega: 195793.4$ rad/sec, outlet perturbation

In turbomachinery noise, several circumferential modes are usually propagated, and therefore the effect of a preferred diagonal direction would have a different effect on each mode, hence worsening the accuracy of the simulation for some of the modes. In order to avoid that, the use of fully unstructured meshes is recommended, trying to minimise the numerical dissipation of the propagation waves due to cell structure.

All the computations shown in this study have been performed using the scalar dissipation model. Therefore limiting the test cases to a range on Mach number of $0.3 < M < 0.7$. However when having very low or high subsonic Mach numbers the matricial dissipation model should be used, that has been already shown by to significantly improve the simulation of propagation of entropy and pressure waves which are more damped when using a more classical scalar model.

One of the critical features involved in the simulation of wave propagation with CFD is the numerical boundary conditions implemented. As recognised by other authors [1], the 1D unsteady non reflecting boundary conditions (UNRBC) are insufficient for an accurate simulation of propagating waves in short domains, and therefore more elaborated boundary conditions are needed. In this investigation, the 1D and 2D UNRBC by Giles [7] have been implemented and their influence on the wave propagation is shown.

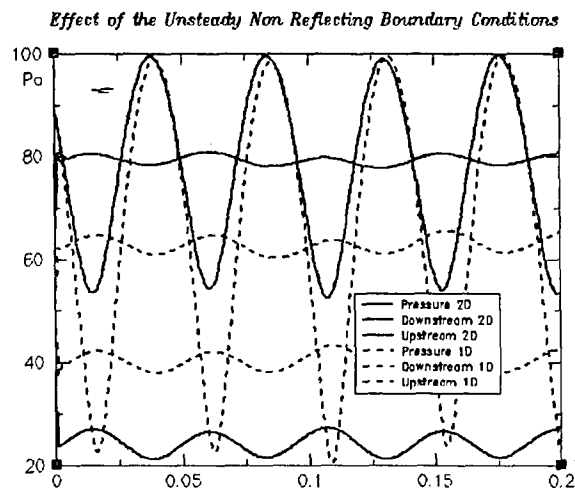


Figure 2: Effect of UNRBC with $\xi: 1.1$, $M: 0.4$

Figure 2 shows that in the case of the 1D non reflecting boundary conditions, the reflection can be up to 60 % of the downstream wave, giving a constructive interference and a pressure field with peak to mean values close to 50 % higher. In all the analysis presented hereafter, 2D non reflecting boundary conditions will be used.

The effect of the cut-off ratio ξ has been investigated through the simulation of different cut-off and cut-on waves. To avoid crossed effects with the mesh definition, all the simulations have been carried out with the same mesh.

For the postprocessing, the wave splitting technique proposed by Wilson [8], has been implemented, which allows to investigate in detail the behaviour of downstream and upstream waves, by means of eigenvalues and eigenfunctions.

Figure 3 shows results of some simulations of waves with $\xi=0.7, 1.1, 3.0$ and 5.0 imposed both in the inlet and in the outlet, with $n_y=80$ points and N_x constant to 320 points

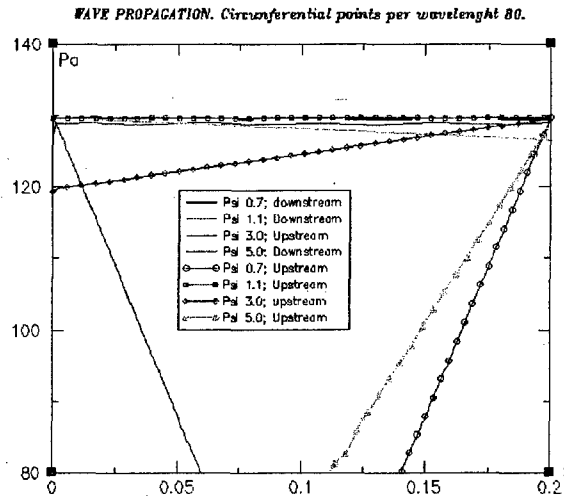


Figure 3: Wave propagation for $\xi: 0.7, 1.1, 3.0, 5.0$ and $n_y: 80$ points. $N_x: 320$ points

As it can be seen, the waves with frequency ratios of 0.7, 1.1 and 3.0 are in general well simulated, with a small axial decay. A cut-off wave as the one with ratio 0.7 is also well simulated, with a linear decay of 0.5237 dB/m for downstream propagating waves and 0.5127 dB/m for upstream propagating waves (versus a theoretical decay of 0.5315 dB/m). Nevertheless, the waves with ξ ratio of 5.0 present deficient prediction. All the simulations have the same circumferential wavelength and number of points per circumferential wavelength n_y but different frequency to have the desired cut-off ratio. This change in frequency changes the propagation characteristics of the wave and therefore a lower number of point per axial wavelength are available as the cut-off ratio increases (for inlet perturbation).

ξ ratio	1.1	3.0	5.0
Points per axial wavelength n_x	3569	40	22.5

Table 1 Points per axial wavelength for $\xi=0.7, 1.1, 3.0, 5.0$ with $N_x=320$ points

Looking at Table 1 and Figure 3 it is shown that the accuracy of the simulation decreases with the number of points per axial wavelength, n_x .

In addition, this accuracy of the wave propagation prediction shown above decreases if a coarser mesh is used for the simulation, with different worsening depending on the ξ ratio (due to the different propagation angles and the resulting number of points per wavelength). This last effect is clearly seen in Figure 4, which shows the results of upstream and downstream running waves for inlet and outlet perturbations with $\xi=3.0$, $n_y=20, 40$ and 80 points per wavelength, and $N_x/N_y=1.0$

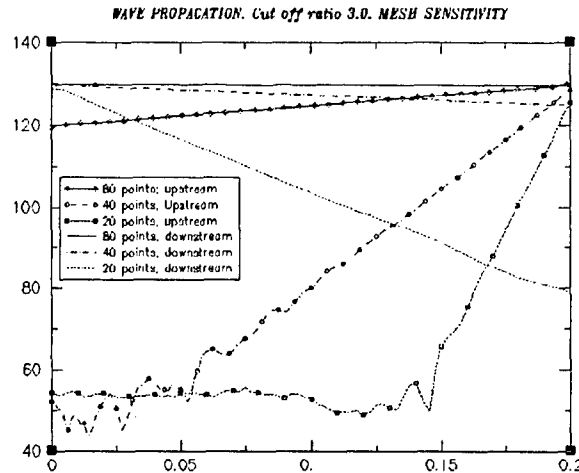


Figure 4: Mesh sensitivity in the simulation of the propagation of a 3.0 cut off ratio wave

The figures shown above illustrate how the numerical results of the wave propagation depend strongly on both the number of points per axial and circumferential wavelength. In an effort to unify the effects of n_y and n_x , Wilson [9] proposed the analysis of wave propagation by means of an average points per wavelength

$$n_{av} = \frac{n_x n_y}{\sqrt{n_x^2 + n_y^2}} \quad (15)$$

parameter that weights the least defined direction.

The analysis of all the simulations computed shows that the dB decay per wavelength depends strongly on the average points per wavelength, in a correlation close to the 3rd order between the error and the points per wavelength. Taking 0.050 dB decay per wavelength as threshold for acceptable accuracy, at least 40 average points are required for the accurate simulation of propagation waves. From this average points per wavelength needed, it raises as the final conclusion that at least 50 points per wavelength in circumferential and axial directions are required for acceptable accuracy.

The effect of the mach numbers in the range $0.3 < M < 0.7$ can be included in the above mentioned analysis, as the damping suffered by a wave (either upstream or downstream potential wave as well as vorticity waves) traversing the physical domain is moderated. In this case, the effect of the mach number will be a change in the axial propagation characteristics of the wave, that can be covered with the mesh analysis performed above.

However, when Mach number is higher than 0.7, demonstrated that upstream potential fields are highly damped due to the slow propagation velocity of such waves. In such a case, the previous accuracy analysis is not valid. In order to overcome this damping, matricial viscosity was implemented in the code, to reduce damping of the upstream running waves. If this matricial viscosity is used, then the accuracy analysis shown before is also valid for high mach numbers. Results of these simulations with the MU^2S^2T code can be found in [6].

4 Flat plate response

After analysing the characteristic parameters of the wave propagation when simulated with CFD codes, the next step is the interaction of a propagating wave with an isolated profile.

Before going into detail of the CFD results, an analysis of the parameters involved in the problem is performed.

The physical characteristics of a flat plate response to unsteady perturbations depend on the following variables

$$\Phi = f(l, t, d, \lambda_y, U_x, U_y, \omega, \rho, T, R_g, \gamma, \mu) \quad (16)$$

that involves longitudes, time, mass and temperature. Taking the pitch distance between blade rows d , the flow velocity U , the speed of sound and R_g for non dimensionalization, the following parameters are found.

$$\Phi = f\left(\frac{l}{d}, \frac{t}{d}, \frac{\lambda_y}{d}, M_x, M_y, St, Re\right) \quad (17)$$

where St stand for the Strouhal number $St = \frac{f \cdot l}{U}$

Tyler and Sofrin first studied the interaction between blade rows [10], showing that ratio of the wavelength to the passage pitch can only take certain values depending on the blade and vane number.

The theory presented in section 2 can be extended to rotor-stator interaction, if the span of the blade rows is small compared with the hub radius, which is a standard approximation in turbomachinery. In this case, the curvature of the duct passage is small, and therefore circumferential direction can be assumed to be the y direction, with

$$\begin{aligned} y &= R \cdot \theta \\ k_{yj} &= m_j \theta \end{aligned} \quad (18)$$

Any unsteady variable take the following form

$$\Phi = \sum \sum A_{n,j} e^{i(\omega_n t + m_j \theta)} \quad (19)$$

The wave field in the stator frame must be invariant when θ is increased the angular pitch of the stator $\Delta = 2\pi/V$ and t is increased by Δ/Ω , due to the unsteady swirling perturbations with angular velocity Ω .

This forces the mode number, m , to be

$$m = kV - nB \quad (20)$$

In the stator frame of reference, the response should be circumferentially periodic with period $\Delta = 2\pi/V$. Imposing that in (19), gives the following expression for the interblade phase angle (IPA).

$$\sigma = -\frac{2\pi B}{V} = -\frac{2\pi d}{\lambda_y} \quad (21)$$

Taking this into account, expression (17) takes the following form

$$\Phi = f\left(\frac{l}{d}, \frac{t}{d}, \sigma, M_x, M_y, St, Re\right) \quad (22)$$

As done in section 3, the Reynolds number will not be taken into account as the study will be limited to potential disturbances.

Within the different profile characteristics, the flat plates present the advantage that a semi-analytical solution of the unsteady response can be obtained with the approach presented by Whitehead [5] by means of a linearized solution of the fluid equations (LINSUB). Therefore, this study will make use of

this results, and the effect of the profile $\frac{t}{d}$ thickness to the pitch length will be left for further studies.

The effect of the Strouhal number has a quite clear physical sense, meaning the ratio between the characteristic time of the unsteadiness, in this case $\frac{1}{f}$ of the incoming wave, and the characteristic time for the fluid to travel along the length of the plate. Results from LINSUB showing this effect on the plate response are shown in Figure 5.

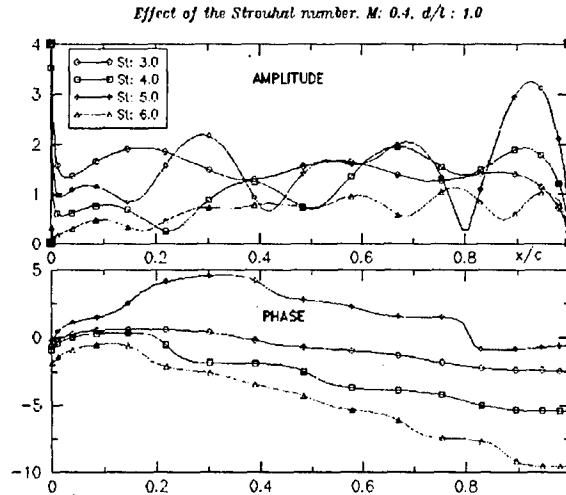


Figure 5: Effect of the Strouhal number St on a flat plate

The number of peaks in the flat plate is approximately equal to the Strouhal number, reflecting that the flow changes St times before leaving the flat plate channel.

However, for low or high mach numbers, this characteristic is distorted due to the compressibility/incompressibility effects. Figure 6 illustrate this effect for perturbations with $St=5.0$ and IPA 270 degrees.

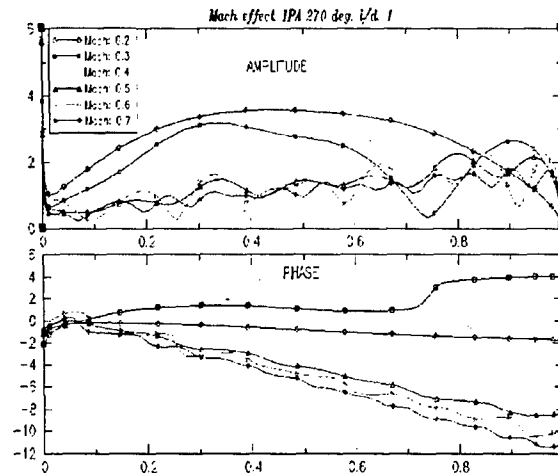


Figure 6: Effect of the Mach number on a flat plate response

The response of the plate at high mach numbers presents more peaks but the peak to mean level of the response is lower, while the opposite behaviour takes place at low mach numbers. This is thought to be due to compressibility effects damping the response while making easier the transmission of pressure waves at high mach numbers.

In (21) was shown that the IPA depends on the number of blades and vanes of the stage. Additionally the IPA also reflects the ratio of the circumferential wavelength of the incoming disturbance to the

distance between the flat plates. The effect of this ratio is shown in Figure 7, for the case of a wave with $\xi=3.0$, and a flat plate cascade of $d/l=1$ and a Strouhal number of 6.836

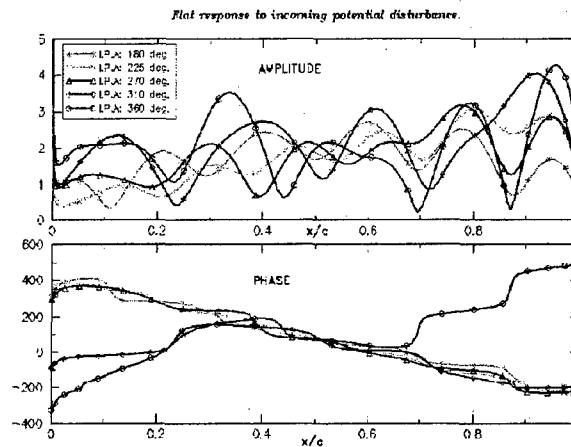


Figure 7: Flat plate response for different interblade phase angles

As previously explained, with $M=0.4$ the amplitude modulation along the blade row presents six peaks for all the interblade phase angle analysed. Nevertheless, as the interblade phase angle of the wave is increased, the peak to mean value of the amplitude modulation increases, to a maximum at 360 degrees. If the phase profile is analysed, it can be seen that the phase modulation is similar in all the cases studied but in the case of 360 degrees, for which a different trend is obtained.

According to Woodley & Peake [11] [12], when unsteady excitations interact with a blade row (either vorticity waves convected due to wakes or downstream-propagating pressure waves) at high frequencies, resonance on the blade row can take place giving a large amplitude response. This kind of behaviour is known as Parker-mode-type resonance, and according to [11] [12], the resonance appears only under certain combination of parameters (Mean flow Mach number, stagger angle, frequency, and blade and vane number).

To test the capability of the codes to simulate the response of the flat plate, a circumferential mode 30 resulting from the interaction of 90 rotating blades with 60 staggered flat plates was computed. The mean flow mach number of 0.4 giving a ξ ratio of 3.0 with an interblade phase angle of 180 degrees. The Strouhal number is set to 6.836 and the pitch to chord ratio to 1.0. In order to ensure a good propagation characteristics, the results from the initial investigation are used to set the grid definition upstream and downstream of the wave.

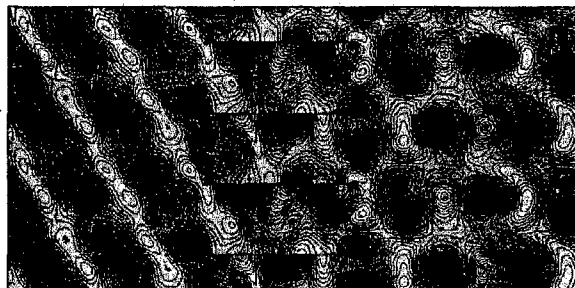


Figure 8: Pressure field for a 60 plates configuration with I.P.A 180°, $M=0.4$, $d/l=1.0$ and $St=8.636$

In Figure 8 the resulting flow field is shown. The wave propagates with an angle close to 75°, impinging in the flat plate. The wave keeps on propagating in the channel between plates and is radiated downstream of the row where multiple interaction between modes gives the complex pattern of the figure.

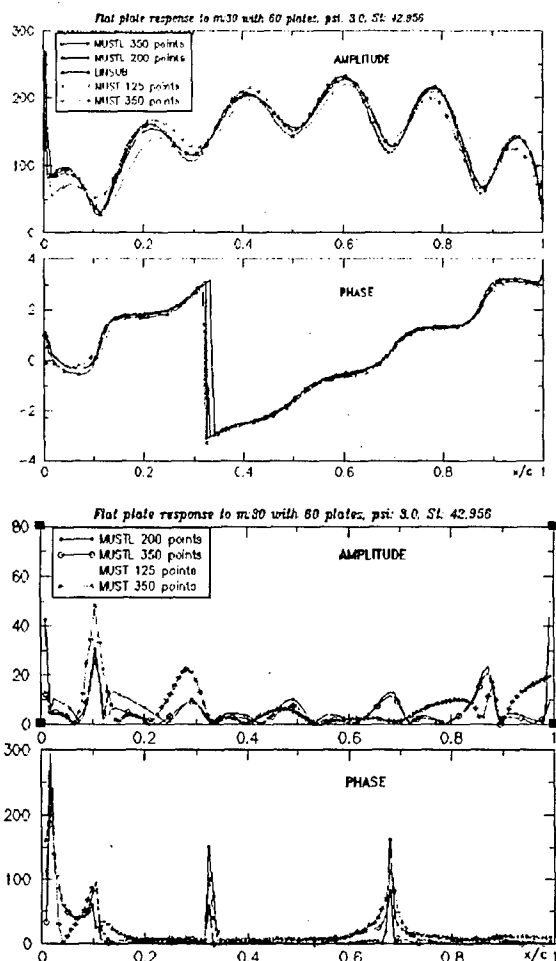


Figure 9: Flat plate response for incoming disturbance with interblade phase angle 180 degrees. Top: Actual Values. Bottom: Percentage Relative Error

The results of the flat plate response are shown in Figure 9.

The top graphic shows how the interaction between the flat plates and the wave is well simulated by both the linear and non linear version of the MU^2S^2T code. The six peaks resulting on the response are reproduced by all the computations, and good agreement with the phase is achieved. The greater differences take place close to the leading edge, probably due to the difficulties on the numerical modelization of the leading edge. Test cases with lower Strouhal numbers have shown lower effects of the boundaries on the plate response. In this case, due to the large Strouhal number, the flat plate response presents high complexity, making the influence of the leading edge significant. In the rest of the plate length, differences are below 10 % of the values predicted by LINSUB, with lower values as the mesh definition is refined. In Figure 9 is also reflected the higher accuracy of the linear with respect to the non-linear version of the code for the same number of points in the flat plate. Table 2 displays the mean error values for the amplitude and phase profiles with respect to the LINSUB value

CASE	Points per Peak	Mean Percentage Error	
		Amplitude	Phase
MUSTL 200 points	33	6.3 %	11.5 %
MUSTL 350 points	58	4.6 %	12.0 %
MUST 125 points	20.8	9.8 %	20.9 %
MUST 350 points	58	7.3 %	17.2 %

Table 2: Mean relative error values of MUST codes with respect of LINSUB as function of the points in the flat plate. Interblade Phase Angle 180 deg

A more complex test case arises from the same perturbation with an interface blade angle of 360 degrees, as presented in Figure 7. In this case, the resonance makes the peak to mean response amplitude larger, while keeping the number of peaks constant with respect to the test case previously shown.

An interblade phase angle of 360° comes from a circumferential mode -30 resulting from the interaction of a 90 blade configuration with 90 flat plates. The Mach number 0.4, with Strouhal number of 6.836 and $d/c=1.0$ are kept as in the previous test case.

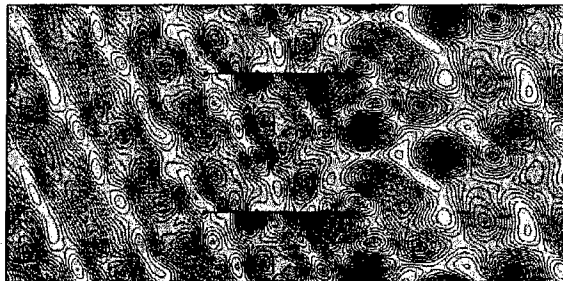


Figure 10: Pressure field for a 90 plates configuration with I.P.A 360, M: 0.4, d/l: 1.0 and St: 8.636

Figure 10 presents the resulting flow obtained. As in the previous test case, the potential wave impinges in the flat plate row with an angle close to 75 degrees. Due to the higher pitch distance between flat plates, the reflection pattern in the channel in between the plates is simpler than in the 180° IPA, with the travelling wave pattern still visible. Radiation downstream of the flat plate row gives a complex field of interactions.

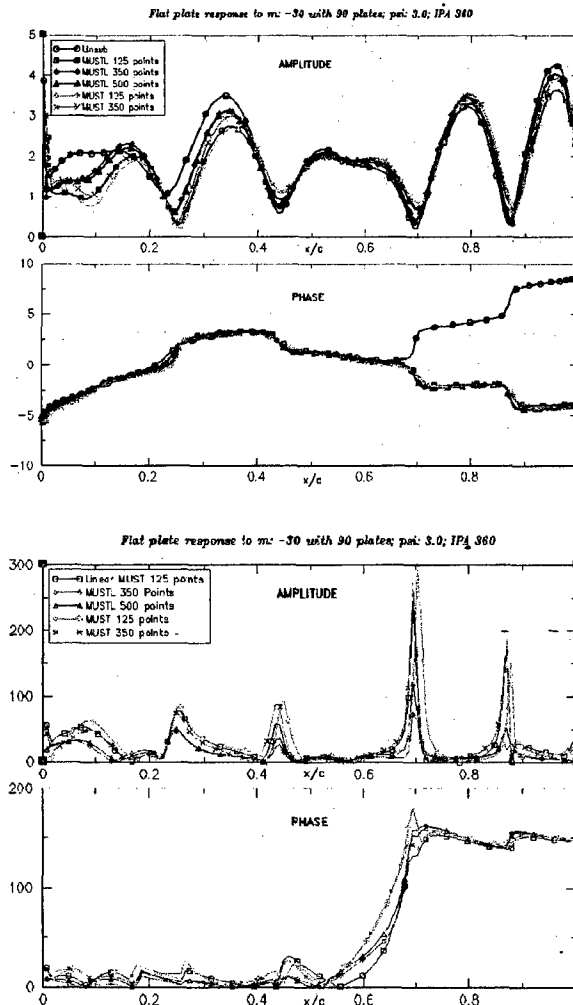


Figure 11: Flat plate response for incoming disturbance with interblade phase angle 360 degrees. Top: Actual Values. Bottom: Percentage Relative Error

The Figure 11 shows the flat plate response compared with the results from LINSUB for the linear and the non linear codes.

The top graphic shows how the interaction between the flat plates and the wave is well simulated by both the linear and non linear version of the MU^2S^2T code, accurately predicting the six peaks of the amplitude response. The differences reported in the area close to the leading edge also appear in all these simulations. Nevertheless, the correct peak to mean value is not reached with none of the simulations, not even with a finer mesh of 500 points in the flat plate.

The phase profile presents great differences in the area of the trailing edge, where none of the simulations is capable to reproduce the results obtained with LINSUB. The change in the trend of the phase variation is a phenomena observed already in other simulations, but that effect was removed with mesh refinement. Nevertheless, in this test case, most likely due to the high complexity of the plate response, the mesh refinement did not help to any improvement on the predictions accuracy.

The relative errors with respect to the LINSUB simulation clearly show how the differences along the plate are low (in the order of 20-25 %), except in the local maxima and minima of the amplitude response, where the relative error presents much larger peaks.

Table 3 displays the mean error values for the amplitude and phase profiles with respect to the LINSUB value

CASE	Points per Peak	Mean Percentage Error	
		Amplitude	Phase
MUSTL 150 points	25	26.2 %	59.8 %
MUSTL 350 points	58	13.9 %	59.1 %
MUSTL 500 points	83	15.5 %	60.1 %
MUST 150 points	25	28.4 %	66.3 %
MUST 350 points	58	26.8 %	65.4 %

Table 3 : Mean relative error values of MUST codes with respect of LINSUB as function of the points in the flat plate. Interblade Phase Angle 180 deg.

It can be seen how in both the linear and non linear versions of the MU^2S^2T code, the relative error decreases when the mesh is refined from 150 to 350 points. Surprisingly, when a very refined mesh with 500 points is employed, a worsening in the solution is found.

In all the simulations both amplitude and phase differences respect to LINSUB predictions are thought to be due to leading and trailing edge simulations. The plate edges effects on the plate response have been pointed out in [11] [12] to play an important role in the resonance behavior of cascades systems.

5 Conclusions

The basic principles of the wave propagation and flat plate interactions simulation have been shown.

It has been demonstrated that both cut-on and cut-off waves can be simulated with CFD codes. In order to ensure a correct modelization of the problem, fully unstructured grids with 2D non reflecting boundary conditions are recommended, since they have shown to have a major impact on the accuracy of the unsteady flow simulation. The main parameter of the accurate wave propagation simulation is the number of points per wavelength, both in circumferential and in axial direction. It has been shown that the effect of Mach number, flow angle, frequency and circumferential mode can be accurately predicted defining sufficient grid points per circumferential and axial wavelength. In case of high Mach numbers, this definition could be not enough to give the desired accuracy, and matricial viscosity should be used.

In the case of unsteady response of flat plates, the driving parameters have been shown. For the range of Mach numbers characteristic of low pressure turbines, the number of amplitude peaks can be determined with the Strouhal number. The amplitude of such response have be shown to be dependent on the interblade phase angle of the wave. Nevertheless, 60 points per response peak have been shown to give a sufficiently accurate response for all the interblade phase angles.

The behaviour of a non linear unstructured Navier Stokes solver for simulating wave propagation and transmission through a flat plate cascade have been studied and the results have been shown to reproduce the same level of accuracy than the linear version of the code (but with some more mesh refinement needed). The necessity of the implementation of 2D UNRBC for minimize the reflections of the wave has also been demonstrated.

6 Acknowledgements

The authors wish to thank ITP for the permission to publish this study and specially the ITP Technology and Methods Department for their support during the project. The authors are acknowledged to Alec Wilson (Rolls Royce) for his support during the implementation of the wave splitting method. This work was partly performed within the TurboNoiseCFD project within the Growth Programme of the European Community.

7 Nomenclature

c: Speed of Sound, m/s
d: Pitch distance, m
k: Wave number
 $k_{n,j}$: Axial eigenvalue, axial wave number, m^{-1}
 $k_{y,j}$: Circumferential eigenvalue, circumferential wave number, m^{-1}
m: Circumferential mode
n: Time harmonic
 n_x : Number of points per axial wavelength.
 n_y : Number of points per circumferential wavelength.
 n_{av} : Average points per wavelength.
l: Profile length, m
t: Profile thickness, m
B: Blade number
CFL: Courant Friedrichs Lewy parameter
M: Mach number
 N_x : Number of points in axial direction
 N_y : Number of points in circumferential direction
R: Radius, m
Re: Reynolds Number
Rg: Gas constant
St: Strouhal number
T: Temperature, K
U: Mean flow velocity, m/s
V: Vane number
 MU^2S^2T : Multirow Unsteady Unstructured Specific Solver for Turbomachinery
 ω : Angular frequency, rad/s
 ω_r : Resonance frequency, rad/s
 λ_x : Axial wavelength, m
 λ_y : Circumferential wavelength, m
 σ : Interface Blade Angle (IPA), deg
 ξ : Cut-off ratio
 ρ : Density, kg/m^3
 γ : Gas Constant
 μ : Viscosity coefficient
 $\sigma\sigma_4$: Artificial viscosity coefficients
 Ω : Shaft rotational speed, rad/s
 Ψ : Unsteady variable
 Δ : Angular pitch, deg.

References

- [1] A. G. Wilson. *Application of CFD to Wake/Aerofoil Interaction Noise- A Flat Plate Validation Case*. AIAA 2001-2135. May 2001.
- [2] F. Kennepohl, G.Kahl, K. Heinig. *Turbine Blade/Vane Interaction Noise: Calculation with a 3D Time-Linearised Euler Method*. AIAA-2001-2152. May 2001.
- [3] B. Lakshminarayana, A. Chernobrovkin, D. Ristic. *Unsteady Viscous Flow Causing Rotor-Stator Interaction in Turbines*. *Journal of Propulsion and Power*. Vol. 16, No, September-October 2000.
- [4] G.A.Gerolymos, D. Vinteler, R. Haugeard, G. Tsanga, I. Vallet. *On the Computation of Unsteady Turbomachinery Flows. Part 2- Rotor/Stator Interaction using Euler Equations*. AGARD CP-571. May 1995.
- [5] D.S. Whitehead. *Classical Two Dimensional Methods. Manual on Aeroelasticity in Axial Flow Turbomachines*, AGARD-AG-298, Vol. 1, Chap. III, 1987
- [6] R. Corral, M.A. Burgos, A. Garcia. *Influence of the Artificial dissipation Model on the Propagation of Acoustic and Entropy Waves*. 45th ASME Gas Turbine and Aeroengine Congress. 8-11 May 2000
- [7] M. B. Giles. *Nonreflecting Boundary Conditions for Euler Equation Calculations*. AIAA Journal, Vol. 28. No. 12, pp 2050-2058
- [8] A. Wilson. *A method for Deriving Tone Noise Information from CFD Calculations on the Aeroengine Fan Stage*. To appear. 2000
- [9] A. Wilson. *TurboNoiseCFD Deliverable 1.6: Review of Generic Studies*. 15 April 2001
- [10] J.M. Tyler, T.G. Sofrin. *Axial Flow Compressor Noise Studies*. SAE Transactions, Vol 70, pp 309-332, 1962
- [11] B.M.Woodley, N. Peake. *Resonant acoustic frequencies of a tandem cascade. Part 1. Zero relative motion*. J. Fluid Mech, Vol 393, pp 215-240, 1999
- [12] B.M.Woodley, N. Peake. *Resonant acoustic frequencies of a tandem cascade. Part 2. Rotating Blade Rows*. J. Fluid Mech, Vol 393, pp 241-256, 1999

Reference # of Paper: 4

Discussor's Name: Dr. Jan Delfs

Author's Name: Mr. Pedro de la Calzada Mazeris

Question:

What is the reason not to use a CAA approach such as that described by Professor Tam?

Answer:

We are primarily interested in the prediction of the tonal noise due to stator-rotor interaction in turbines. For that, we need to solve first for the aerodynamics in order to accurately simulate the effect of both the potential field and the vortical wake convection. Our intention is to reduce the number of codes used in the simulation of the unsteady aero thermal behavior of turbine stages. Therefore we are concentrating our efforts to have only one code with the necessary features implemented to predict the unsteady and steady flow fields. We have updated our CFD code for the steady aero-thermal field in turbines and we want to keep this experience and improve the base code further. Therefore we are working on the code in the direction of CAA by improving the boundary conditions and the artificial viscous damping.

Additionally, the modes and frequencies in which we are interested have long wavelengths on the order of the pitch in the circumferential direction. Thus, the mesh refinement needed to resolve the viscous boundary layer and wakes is probably finer than that needed to resolve the acoustics. So, we are happy to solve for the unsteady behavior with the same mesh and code we use for the steady aero-thermal field.

Discussor's Name: Mr. Jose M. Riola Rodriguez

Author's Name: Mr. Pedro de la Calzada Mazeris

Question:

How long does the nonlinear code take to run compared to the linear version?

Answer:

We have found a factor of two between the two codes. In order to have an idea of the total time needed for the flat plate cases presented here: for a mesh with around 20,000 nodes, the linear version runs overnight and the nonlinear version needs a full day.